Journal of Insect Science, (2024) 24(4): 16; ieae074
https://doi.org/10.1093/jisesa/ieae074
Research

ENTOMOLOGICAL SOCIETY OF AMERICA
SHARING INSECT SCIENCE GLOBALLY

OXFORD

A mountain pine beetle (Coleoptera: Curculionidae) adult development rate model confirms evolved geographic differences

Catherine E. Wangen[1], James A. Powell[1,*], Barbara J. Bentz[2]

[1]Department of Mathematics and Statistics, Utah State University, Logan, UT 84322, USA, [2]USDA Forest Service, Rocky Mountain Research Station, Logan, UT 84321, USA *Corresponding author, email: jim.powell@usu.edu

Subject Editor: Brian Aukema

Received on 16 February 2024; revised on 16 May 2024; accepted on 5 July 2024

Insects live in a wide range of thermal environments and have evolved species- and location-specific physiological processes for survival in hot and cold extremes. Thermally driven dormancy strategies, development rates and thresholds are important for synchronizing cohorts within a population and to local climates and often vary among populations within a species. Mountain pine beetle (MPB), *Dendroctonus ponderosae* Hopkins (Coleoptera: Curculionidae, Scolytinae), is a widely distributed forest insect native to North America with clinal genetic differentiation in thermally dependent traits. MPB development occurs in *Pinus* phloem beneath the bark, and its cryptic habitat makes experimentation difficult, particularly for the adult stage. We describe a novel method for modeling MPB adult development following pupation and terminating in emergence from a brood tree. We focus on an Arizona (southern) MPB population with previously described preadult development rates. Field-observed tree attack, adult emergence, and phloem temperature data are combined in a parameterized cohort model and candidate rate curves are evaluated to describe adult emergence timing. Model competition indicates that the Brière rate curve provided the best fit to field data and performed well under cross-validation. Results confirm that the development of Arizona MPB adults is slower than the previously described development rate of more northern Utah adults. Using the estimated adult rate curve in a scenario of increasing mean temperatures, we show that the timing of second-generation adult emergence in the same year would result in cold-intolerant lifestages during winter, limiting the success of bivoltine populations.

Key words: Dendroctonus ponderosae, teneral adult, model, phenology, rate curve

Introduction

Insects are among the most abundant animals worldwide, living in a wide range of thermal habitats. Because insect body temperature is dependent on the ambient environment, species- and location-specific physiological processes have evolved that promote survival, fitness, and reproduction. Multiple adaptations are used to protect against thermal extremes, hot and cold, including developmental strategies to optimize physiological energy requirements and synchronize the timing of thermally sensitive life stages. Common physiological processes include dormancy (i.e., diapause and quiescence) and development rates and thresholds. Diapause and quiescence are resting states that can both synchronize cohorts and facilitate survival in adverse conditions such as extreme heat or cold by suppressing metabolism and respiration (Tauber and Tauber 1986, Denlinger 2002). Development rates and lower thermal thresholds allow individuals to pause development when temperatures are suboptimal. By limiting the development of individuals in some life stages while others develop, thermal thresholds can help synchronize cohorts (Gurney et al. 1994, Grist and Gurney 1995). These physiological processes can vary among species and among life stages and populations within a species (Danilevskii 1965, Masaki 1980, Honek 1996). The potential for adaptive differentiation in these types of environmentally determined traits complicates predicting demographic consequences in a changing climate, particularly for species with a broad geographic distribution.

Due to its economic and ecological impact, extensive research has been conducted on thermally dependent traits of the mountain pine beetle (MPB, *Dendroctonus ponderosae* Hopkins [Coleoptera: Curculionidae, Scolytinae]), a widely distributed native forest insect that attacks and can kill trees within multiple *Pinus* species across western North America. Thermally dependent traits that synchronize cohorts are important for MPB because adults must attack a host simultaneously to overwhelm host defenses and successfully colonize, reproducing in the inner bark (phloem). Phloem temperatures directly but nonlinearly affect MPB progress through the stages of their life cycle, which have varying temperature thresholds (Bentz

et al. 1991, Powell and Logan 2005). These thresholds allow MPB to be most successful in a thermal niche where they are univoltine (1 generation in a year) and adult emergence is seasonally appropriate and synchronized (Logan and Bentz 1999, Logan and Powell 2001). Semivoltine (1 generation in 2 years) cohorts can be found at high elevations and in cold years, although the extended generation time and potential cohort asynchrony and winter mortality limit population growth and survival (Safranyik and Linton 1991, Bentz et al. 2014). In addition, locally adapted facultative diapause in the prepupal stage (Bentz and Hansen 2018) can also facilitate emergence synchrony and increase the likelihood of overwintering as a cold-tolerant larval instar (Bentz and Mullins 1999) rather than a cold-intolerant pupae (Bleiker and Smith 2019). The prepupal MPB diapause, however, also reduces the chance for successful bivoltine (2 generations in 1 year) cohorts, a voltinism that has rarely been observed within MPB's native range (Bentz and Powell 2014, Bentz et al. 2014, Soderberg et al. 2021) (but see Mitton and Ferrenberg 2012).

Accurately predicting thermally driven changes in life cycle timing requires determining how the aggregation of heat energy contributes to completing development in each stage of an insect's development. The idea of integrating temperature through time to predict life history events dates back to the degree day model of de Reamur in 1735, in which the development rate is assumed to be linear above a temperature threshold (Bonhomme 2000). In more recent times, empirical non-linear models, such as the logistic equation of Davidson (Davidson 1944), the matched asymptotic curves of Logan et al. (1976), and the Briere curve (Brière et al. 1999), improve upon degree day models by incorporating nonlinearity at high and low-temperature thresholds. While details of thermal response vary among rate curves, they all provide a way to sum developmental response to varying temperatures over time and predict the timing of observable life history events. Typically, rate curves are parameterized by fitting to laboratory observations of the time required for development to complete in individual life stages at a variety of constant temperatures (see, for example, Rebaudo and Rabhi 2018). Given a temperature record in the natural environment, fitted developmental rate curves can forecast emergence distributions using numerical integration to track the development of ovipositional cohorts over time (Régnière and Powell 2013).

Despite extensive research on MPB, predicting demographic consequences across its range is complicated because populations are locally adapted with clinal genetic differentiation in thermally dependent traits. In common garden experiments (Bentz et al. 2001, Bracewell et al. 2013, Soderberg et al. 2021), the generation time of a southern latitude population in Arizona (AZ) was found to be significantly longer than that of a more northern population in Utah (UT), suggesting an extended development time in one or multiple life stages of southern populations. McManis et al. (2018) investigated developmental parameters of an AZ MPB population and found that parameters for eggs, 4 larval instars, and pupae varied from those of more northern US latitude MPB populations, as described in Regniere et al. (2012), but not sufficiently to account for the overall difference in observed generation time. Following pupation, teneral adults spend time until maturation, feeding on associated mycangial fungi (Addison et al. 2015) before emerging from the host tree as mature adults. The results of McManis et al. (2018) and Soderberg et al. (2021) suggest that the development rate of the adult stage, either teneral or mature or both combined, in AZ MPB populations is lower than in more northern MPB populations. Standardized experimental protocols for describing development rates of preadult lifestages of this cryptic insect (i.e., "phloem sandwiches," Bentz et al. 1991, McManis et al. 2018); however, have proven to be insufficient for observing development rates and maturation of the teneral adult and timing of mature adult emergence from a tree. Predicting migration and extinction potential for this key forest disturbance agent in a changing climate (Bentz et al. 2019) will be improved with the development of geographic-specific mechanistic models with well parameterized descriptions of the adult stage.

Our goal is to model developmental timing for the cryptic MPB teneral and mature adult stages of a 'southern' (i.e., central AZ) MPB population by combining field-observed data on tree attacks, adult emergence, and phloem temperatures with previously determined development rates for oviposition, eggs, 4 larval instars, and pupae. We first review previously developed rate curves for preadult life stages (McManis et al. 2018, Wangen et al. 2022), in addition to a cohort-based model used to describe progression through the lifestages (Gilbert et al. 2004). Adult development rate curves are parameterized by integrating preadult rate curves and unparameterized, candidate adult curves with field-observed data and phloem temperatures. The best curve is selected by comparing nominal and bootstrapped Akaike Information Criterion (AIC) values, and the resulting model is evaluated using additional field data. We compare the estimated development rate for the AZ population to previously published information on the more northern (UT) adult development rates. Using the developed model, we also examine the potential for bivoltinism in the AZ MPB population by increasing mean temperatures and applying previously described constraints on lifestage survival and seasonality.

Materials and Methods

Observed Phloem Temperature, MPB Attacks and Adult Emergence

Our study site was a *Pinus strobiformis* Engelmann (Pinales, Pinaceae) stand at Lockett Meadows, Coconino National Forest, near Flagstaff, AZ. Phloem temperatures and the number and timing of adult MPB attacks and emerging brood adults the following year were collected on multiple trees from 2015 to 2017. Two full MPB generations were observed over 2 years (2015/2016, 2016/2017), indicating a univoltine lifecycle at this site. Phloem temperatures were measured at hourly intervals (Campbell Scientific, Logan, UT, USA) for the north and south aspects of multiple tree boles. North and south aspects were differentiated because previous field data indicated that the southern aspect of a tree bole often has an increased mean temperature due to insolation, which may cause significant differences in fitness and developmental traits for individuals collected from different aspects (Bentz et al. 2014). Phloem temperatures were recorded for the duration of MPB attacks, brood development, and adult emergence on 3 trees from 4 June 2015 through adult emergence in 2016 and on 3 additional trees from 9 August through adult emergence in 2017.

To ensure MPB attacks on temperature-probed trees, an MPB pheromone bait (Synergy Semiochemicals Corporation, BC, Canada) was attached to each tree on the north bole aspect at 1.4 m from the ground. Tree baits were removed a week later after 10–15 attacks were observed on the tree. Once attacks were initiated, they were monitored every other day around the entire circumference of each tree bole from 0.3 to 1.5 m above the ground. On each observation day, the entire sample space was surveyed, counting attacks that were indicated by either frass or resin exuding from entry holes. A permanent marker was used to mark each attack so that it would not be counted more than once. Attacks were monitored until no new attacks were observed for 2 consecutive observation days.

Observations occurred at intervals of 2–4 days, without differentiation between bole aspects. Thus, all attacking beetles from the end of the previous observation to the current observation were included in a day of attack. At the end of the attack season emergence cages, 31 cm × 61 cm in size and constructed from flexible nylon screen with a mesh size sufficiently small to prevent adult beetle escape, were stapled to the north and south bole aspects centered at 1.4 m. The following year adult emergence was counted separately for the north and south aspects of trees at 2–6 day intervals. Similar to attack data, all emerging beetles from the end of the previous observation to the current observation were included on a single day.

Model Development

To describe a developmental rate curve for the cryptic adult stage of the AZ population, we incorporate (i) a novel oviposition model (Wangen et al. 2022) and a new method of calculating the time delay (egg-free gallery construction) before oviposition, (ii) preadult development rates estimated for the AZ MPB population (McManis et al. 2018), (iii) a previously developed MPB cohort model describing progression through preadult lifestages (Gilbert et al. 2004), and (iv) several candidate development rate curves for the adult stage. An important aspect of oviposition is that variability occurs not only in oviposition rate but also in fecundity; both effects are included in the Wangen et al. (2022) oviposition model. The oviposition model was used as input to the cohort model, based on parameters in McManis et al. (2018), incorporating lifestage-specific-rates and known effects of variability. Field-observed MPB attacks and phloem temperatures at the Lockett Meadow site were used with the oviposition and cohort model; candidate adult rate curves were then fit to observe adult emergence. We review previously described models and parameters for the AZ population and then describe the likelihood framework relating to predicted and observed adult emergence from a tree. Finally, we determine a suitable teneral adult rate curve and distribution of deviance from observations by maximizing the likelihood.

Oviposition and Gallery Construction

There is a time period after MPB mating during which the female excavates phloem but has yet to begin oviposition, we denote by t_o. This egg-free gallery length may help MPB avoid the induced resin response of the host tree. We parameterize a rate curve for the preoviposition stage by minimizing the sum squared error for laboratory data of MPB development at constant temperatures (see Wangen 2021). The rate curve used by McManis et al. (2019) is

$$r_0(T) = \psi\left[e^{\omega(T-T_b)} - \left(\frac{T_m - T}{T_m - T_b}\right) e^{-\frac{\omega(T-T_b)}{\Delta_b}} - \left(\frac{T - T_b}{T_m - T_b}\right) e^{\omega(T_m-T_b)-\frac{T_m-T}{\Delta_m}}\right], \quad (1)$$

with $r_0(T) = 0$ for $T \notin (T_b, T_m)$. Here T_m and T_b correspond to the upper and lower temperature transitions from normal to negligible development at the upper and lower thresholds, ω describes the expected exponential acceleration of rate with temperature, and ψ is proportional to the maximum development rate. The parameters Δ_m and Δ_b are the width of the thermal transitions near the upper and lower thresholds. Parameters for the time required to produce the egg-free gallery appear in Table 1.

After the construction of the egg-free gallery, oviposition begins. Wangen et al. (2022) show that the probability of oviposition the fth quantile of eggs, given an attack date τ, is distributed in time

$$p_{ovi}(t|\tau, f) = \frac{1}{\sqrt{2\pi\sigma^2}} e^{-\left(\frac{\ln(f)+R(t,t_0+\tau)}{t-t_0}\right)^2/2\sigma^2} \left|\frac{-(\ln(f) + R(t, t_0+\tau))}{(t-t_0)^2} + \frac{r_0(T(t))}{t-t_0}\right|, \quad (2)$$

where t_0 is the time delay before oviposition, and $R(t, t_0+\tau)$ is the integral of oviposition rates from $t_0+\tau$ to t. Integrating across quantiles gives the resulting distribution of eggs for a given attack day,

$$p_{ovi}(t \mid \tau) = \int_0^1 p(t \mid \tau, f)\ df. \quad (3)$$

For any individual tree, there are multiple attack dates, τ, each with a corresponding number of attacks, $A(\tau)$. The resulting density of eggs for any particular day, t, is therefore

$$p_{egg}(t) = \int_{\tau_{min}}^{\tau_{max}} A(\tau)\, p_{ovi}(t|\tau)\quad d\tau. \quad (4)$$

Individual distributions are determined computationally for an observed attack date, τ, by calculating t_0 using hourly phloem temperature as input to the rate equation (1). Hourly rates are summed into daily rates, and a cumulative approximation to the integral is calculated using trapezoidal quadrature. Cumulative differences of one from start date T determine the time at which the egg-free distance is completed.

For oviposition, distributions for specific values of f, beginning at $\tau + t_0$, are calculated using equation (2). Cumulative rates are computed using the trapezoid rule on ovipositional rates, then each PDF is then normalized. The process is repeated for f = 0.05, 0.10,..., 0.095 and the oviposition density (3) approximated using trapezoidal quadrature in f. Complete details of derivation and calculation appear in Wangen et al. (2022).

Parameterized AZ MPB Development Curves for Preadult Lifestages

McManis et al. (2018) obtained rate curve parameters for AZ MPB lifestages using phloem sandwiches in the lab. The development of

Table 1. Egg-free gallery parameters found in Wangen et al. (2022) and life stage parameters for a southern population of MPB found by McManis et al. (2018, 2019)

Lifestage	Ψ	ω	Tb	Tm	Δb	Δm	σ
Egg-free gallery	0.177	0.0632	5.90	29.6	2.55	2.73	–
Oviposition	0.0913	0.0309	6.60	30.9	1.36	1.99	0.320
Eggs	0.0326	0.205	6.025	31.9	0.541	5.50	0.038
1st instar	0.0521	0.152	4.60	31.8	0.0117	5.43	0.218
2nd instar	0.0431	0.137	5.98	31.8	0.0413	4.45	0.152
3rd instar	0.017	0.186	6.01	31.3	0.0	4.31	0.165
4th instar	0.0545	0.169	15.0	31.4	0.0	5.29	0.135
Pupae	0.0166	0.166	6.35	30.8	0.0	3.54	0.0673

individuals from egg to pupation was monitored daily at a range of constant temperatures, and duration was recorded for each lifestage. Normal variability in rates for all lifestages was observed, and estimated parameters fit to the rate curve (1) appear in Table 1. Duration of the teneral and mature adult lifestages, which terminate in emergence from a tree, is difficult to measure with the phloem sandwich method and was not modeled by McManis et al. (2018).

Extended von Foerster Cohort Model

Output of the oviposition model is used as input for the egg-to-pupae cohort model utilizing the parameters from McManis et al. (2018). While some types of phenology models focus exclusively on the development of a median individual (Régnière and Powell 2013), this ignores the intrinsic variability of rates in a population. A cohort model provides an efficient way to incorporate the variability in rates over time for individuals in the cohort. McManis et al. (2018) determined that observed rates had normal variance, which allows us to use the Extended von Foerster (EvF) equation developed by Gilbert et al. (2004),

$$\frac{\partial}{\partial t}u_j(a,t) + r_j[T(t)]\frac{\partial}{\partial a}u_j(a,t) = \frac{1}{2}\sigma_j^2\frac{\partial^2}{\partial a^2}u_j. \quad (5)$$

Here j is the developmental lifestage index, $u_j(a,t)$ is the population density at time t and age a (normalized such that $0 \leq a \leq 1$), $r_j[T(t)]$ is developmental rate at temperature $T(t)$, and σ_j^2 is the variance in development for life stage j. The density, $u_j(a,t)$, and emergence distribution, $p_j(t)$, are related by $p_j(t) = u_j(a=1,\ t)$. The EvF equation reflects the mixing of individuals aging slower and faster than the mean, creating an effective diffusion among ages. The Green's function solution,

$$p_j(t) = \int_0^\infty p_{j-1}(\tau)\frac{e^{\frac{-(1-\int_\tau^t r_j(T(s))ds)^2}{2\sigma_j^2(t-\tau)}}}{\sqrt{2\pi\sigma_j^2(t-\tau)^3}}\left|1-\int_\tau^t r_j(T(s))\quad ds\right|\quad d\tau, \quad (6)$$

projects emergence distributions of life stages following oviposition, using $p_0(t) = pegg(t)$ (Powell and Bentz 2009). Parameters for an AZ MPB population (Table 1) are used for the egg, 4 larval instars, and pupal stage rate curves. Equation (6) is evaluated numerically using hourly development rates and trapezoidal quadrature.

Potential AZ MPB Adult Development Curves

For the unknown development rate of the cryptic adult stage, we consider 5 rate curves of varying complexity. Adult emergence predicted using competing rate curves is compared with field observations to determine which candidate curves are most descriptive. Where feasible, we rescale curves to estimate the maximum developmental rate directly.

Logistic

The first adult curve is based on the logistic equation of Davidson (1944),

$$r_{logistic}(T) = \frac{r_{max}\cdot e^{(T-T_C)/\Delta_b}}{1+e^{(T-T_C)/\Delta_b}} \quad (7)$$

which plateaus at a peak developmental rate of r_{max}. The parameter T_C specifies the developmental threshold and Δ_b determines the sensitivity to that threshold. To reflect the upper thresholds seen in MPB development, we adjust (7),

$$r_{logmax}(T) = r_{max}\left[\frac{e^{(T-T_b)/\Delta_b}}{1+e^{(T-T_b)/\Delta_b}} - \frac{e^{(T-T_m)/\Delta_m}}{1+e^{(T-T_m)/\Delta_m}}\right]. \quad (8)$$

Here T_b and T_m are the lower and upper-temperature thresholds, while Δ_b and Δ_m determine the sensitivity of those thresholds.

Brière

The rate curve developed by Brière et al. (1999) is

$$r_{Brière}(T) = \psi\frac{T}{T_m}\left(\frac{T}{T_b}-1\right)\sqrt{1-\frac{T}{T_m}} \quad (9)$$

for $T_b < T < T_m$, with $r(T) = 0$ for $T \notin (T_b, T_m)$. Here T_m is the upper temperature threshold, T_b, is the lower temperature threshold, and ψ controls the peak rate. To facilitate comparison, we rescale the curve so that maximum rate of development, r_{max}, can be parameterized directly. The optimal temperature, T_{opt}, is calculated using Brière et al. (1999) equation (8). We define a normalizing constant,

$$N = T_{opt}(T_{opt}-T_b)\sqrt{1-\frac{T_{opt}}{T_m}}, \quad (10)$$

and rewrite Equation (9)

$$r_{BrièreMax}(T) = r_{max}\cdot\frac{T}{N}(T-T_b)\sqrt{1-\frac{T}{T_m}}. \quad (11)$$

Logan

The rate curve developed by Logan et al. (1976), often used for describing bark beetle species phenology (e.g., Hansen et al. 2011, Davídková and Doležal 2019), is

$$r_{Logan}(T) = \psi\left[e^{\omega(T-T_b)} - 1 - \left(e^{\omega(T_m-T_b)}-1\right)e^{-(T_m-T)/\Delta_m}\right] \quad (12)$$

For $T_b < T < T_m$, with $r(T) = 0$ for $T \notin (T_b, T_m)$. Here T_m is the upper temperature threshold, T_b, is the lower temperature threshold, and ψ controls the peak rate, ω controls the rate acceleration at lower temperatures, and Δ_m is the thickness of the upper threshold boundary layer. We calculate r_{max} and T_{opt} computationally for the Logan curve after fitting.

Piecewise Linear Rates

We also use 2 rate curves based on piecewise linear functions, which are "nonparametric" (NP) in the sense that the unknown free constants are directly interpretable as rates at specific temperatures, as opposed to indirectly influencing the shape of developmental curves through a smooth function. The simpler, triangular curve, referred to as nonparametric curve 1 (NP1), has a minimum temperature threshold T_b, a maximum temperature threshold T_m, a maximum rate r_{max}, and an optimal temperature T_{opt} at which r_{max} occurs (Supplementary Fig. S1A). The second curve (NP2) includes an additional temperature break point, $T_1 < T_{opt}$, where the rate is equal to r_1, with $r_1 < r_{max}$ (Supplementary Fig. S1B).

Fitting Rate Curves to Adult Emergence Data

Adult rate curves are parameterized using MPB adult emergence data collected at Lockett Meadows, AZ. Observations of MPB emergence were recorded every 2–4 days. The total number of observed beetles for a tree side i is the sum of beetles that emerged on that side, N_i. The predicted emergence between observation days t_{k-1} is weighted by the total number of beetles observed emerging,

$$\text{pred}_{i,k} = N_i\int_{t_{k-1}}^{t_k} p_8(t)\quad dt. \quad (13)$$

Due to a lack of tree attacks and/or emergence only 3 of the 6 trees monitored were suitable for inclusion in the analyses. Attack and emergence data from 2 trees (Tree 1, 2016–17 and Tree 2,

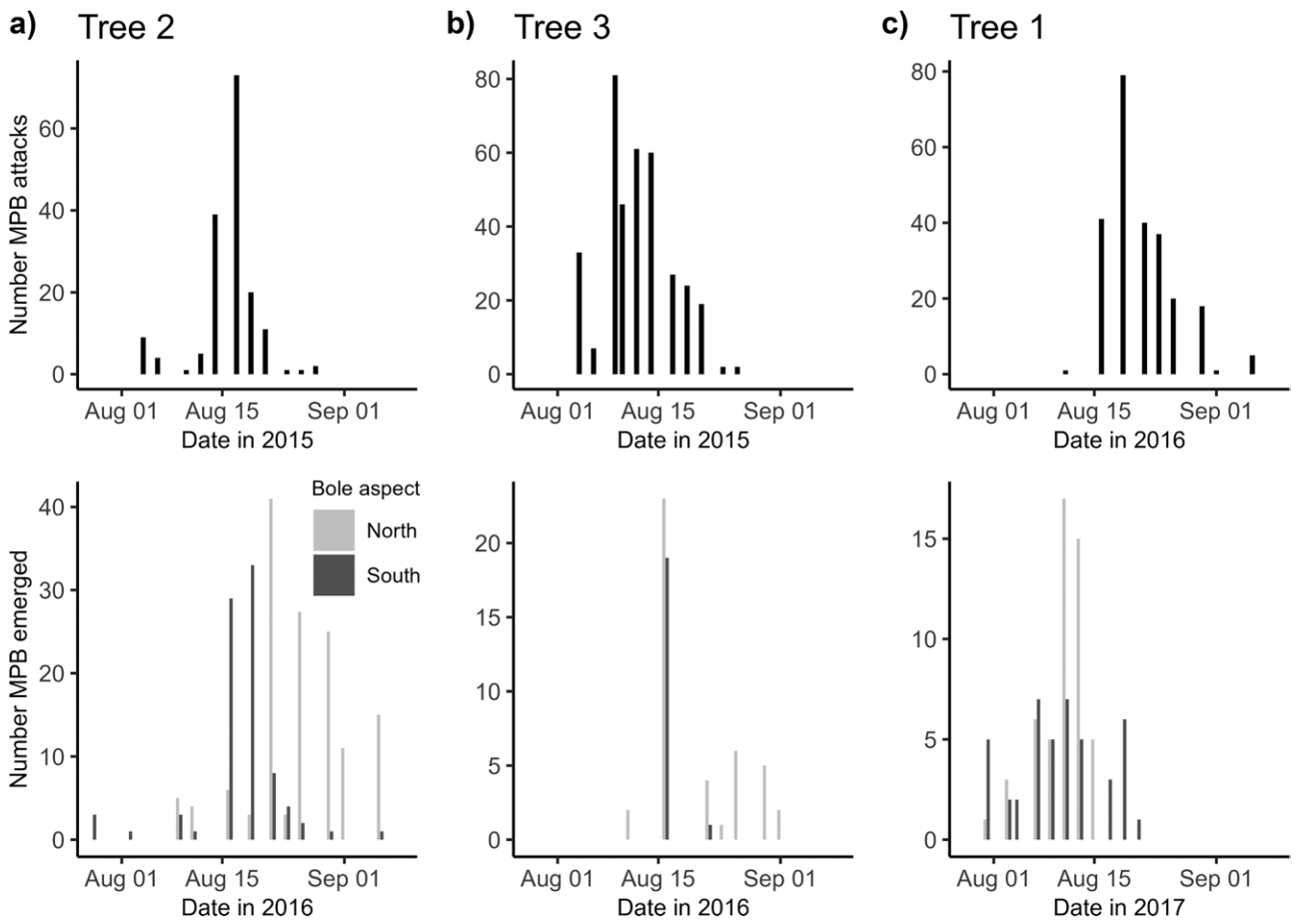

Fig. 1. Number of MPB attacks (top) and adults emerged the following year by north and south bole aspect (bottom) for A) Tree 2, B) Tree 3, and C) Tree 1.

2015–16) were used for parameterization and cross-validating the model, and emergence data from Tree 3 (2015–16) was used for model evaluation (Fig. 1).

Determining Appropriate Distributions for Deviance

To determine the best error model for the deviance between predicted and observed adult emergence, we calculate the negative log likelihood (NLL) using Normal, Laplace, and Poisson distributions. For given data and a candidate rate curve, parameters for rate curves and error distributions are determined by minimizing NLL computationally. The AIC (Burnham 2002),

$$\mathrm{AIC} = 2 \quad \mathrm{NLL} + 2p, \tag{14}$$

where p is the number of fitted parameters (including those in the error distribution), is used to allow deviance models to compete on an equal footing. A lower AIC represents a more competitive model due to a smaller NLL (larger overall likelihood). However, the AIC also penalizes for overfitting with more complex models because it increases with the number of parameters. In preliminary investigations, the Brière rate curve for adults had the best fit to nonbootstrapped data, as measured by AIC values across trees and error models, and is therefore used to determine the most suitable deviance distribution.

Laplace Deviance Distribution

If the errors have a Laplace distribution, for a single observation, $\mathrm{obs}_{i,k}$, on side i on day k,

$$\mathrm{Prob}\left(\mathrm{obs}_{i,k} \mid \mathrm{pred}_{i,k}\right) = \frac{1}{2\alpha_i} \exp\left[-\frac{\left|\mathrm{obs}_{i,k} - \mathrm{pred}_{i,k}\right|}{\alpha_i}\right], \tag{15}$$

where α_i is an additional parameter specifying the variance. The NLL function for a single tree is then

$$\mathrm{NLL} = \sum_i \sum_k \left[\log\left(2\alpha_i\right) + \frac{1}{\alpha_i}\left|\mathrm{obs}_{i,k} - \mathrm{pred}_{i,k}\right|\right]. \tag{16}$$

Normal Deviance Distribution

If the errors have a Normal distribution, for a single observation on a tree,

$$\mathrm{Prob}(\mathrm{obs}_{i,k}|\mathrm{pred}_{i,k}) = \frac{1}{\sqrt{2\pi\sigma_i^2}} \exp\left[\frac{-\left(\mathrm{obs}_{i,k} - \mathrm{pred}_{i,k}\right)^2}{2\sigma_i^2}\right], \tag{17}$$

where σ_i^2 is the variance. The NLL function for a single tree then becomes

$$\mathrm{NLL} = \sum_i \sum_k \left[\frac{1}{2}\log\left(2\pi\sigma_i^2\right) + \frac{1}{2\sigma_i^2}\left(\mathrm{obs}_{i,k} - \mathrm{pred}_{i,k}\right)^2\right]. \tag{18}$$

Poisson Deviance Distribution

If the errors have a Poisson distribution, for a single observation on a tree,

$$\mathrm{Prob}(\mathrm{obs}_{i,k}|\mathrm{pred}_{i,k}) = \frac{e^{-\mathrm{pred}_{i,k}}\left(\mathrm{pred}_{i,k}\right)^{\mathrm{obs}_{i,k}}}{\mathrm{obs}_{i,k}!} \tag{19}$$

for the kth observation on tree side i. The NLL function for a single tree is then

$$\mathrm{NLL} = \sum_i \sum_k \left[\mathrm{pred}_{i,k} - \mathrm{obs}_{i,k} \log\left(\mathrm{pred}_{i,k}\right) + \log\left(\mathrm{obs}_{i,k}!\right)\right]. \quad (20)$$

Computation and Bootstrapping

Errors and AIC are calculated by using the MATLAB fmincon function to minimize NLL on bootstrapped emergence data. Bootstrapping is performed by randomly selecting 1500 samples, with replacement, considering each individual adult beetle, as well as any day with no emergence recorded, as observations to be resampled.

Results

MPB attacks and adult emergence occurred between early August and mid-September both years on the 3 trees that were suitable for use in model development and evaluation (Fig. 1). Phloem temperatures showed a strong seasonality with an over 30 °C change between summer and winter (supplementary Fig. S2A). South bole aspect temperatures were warmer during the day than north bole aspect temperatures (Supplementary Fig. S2B), with a mean maximum temperature difference varying between 0 and 7 °C (mean 2.00 with

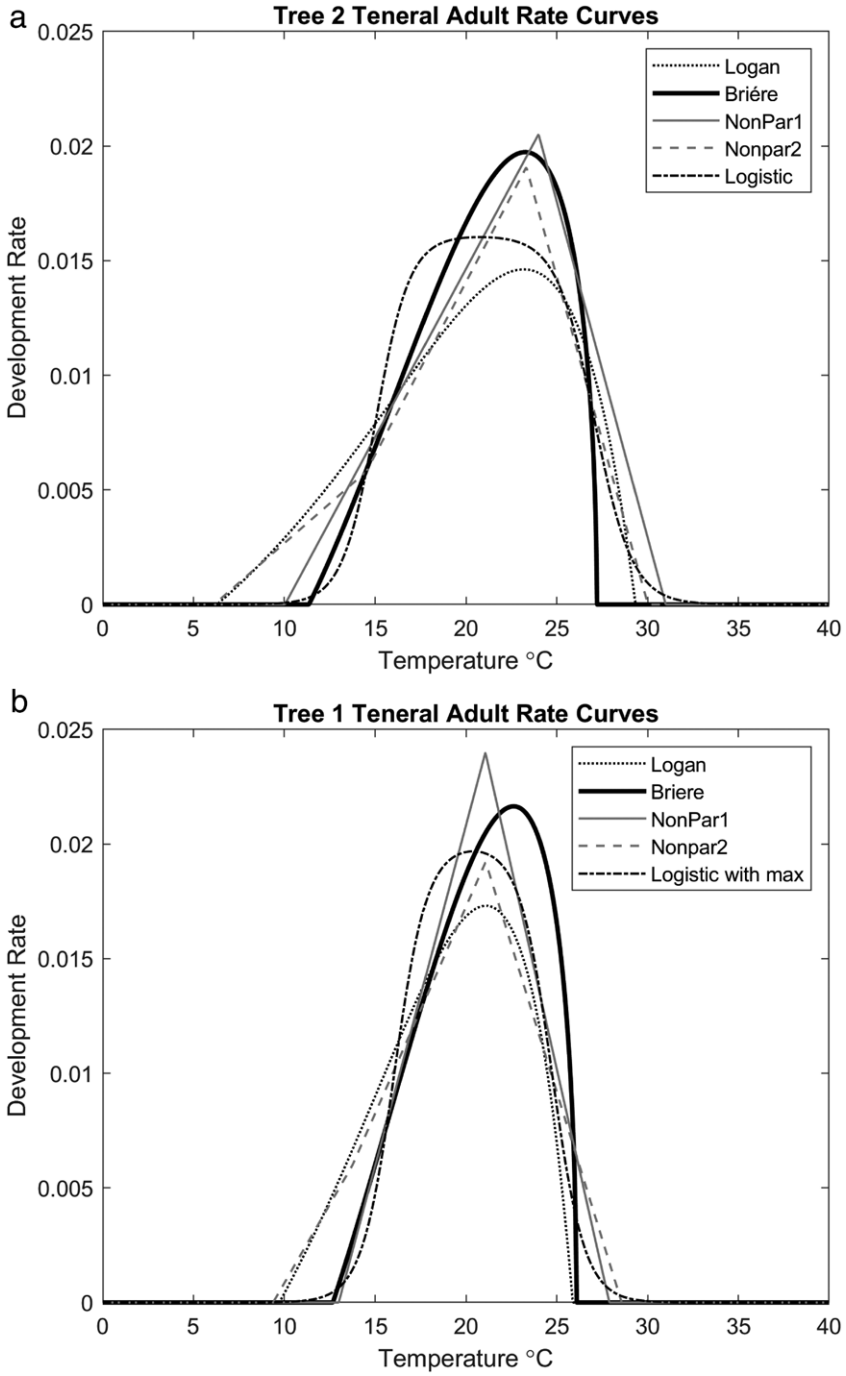

Fig. 2. Five potential adult development rate curves fit for A) Tree 2 and B) Tree 1. The curves share inflection points at near 15 and 27C, and the Brière curve has the lowest nominal AIC value for both trees.

Table 2. Parameters for Tree 2 adult development rate curves. The estimated variance of development rates is given by σ. We calculate $r_{max} = 0.0146$ for the Logan curve (not an estimated parameter for this curve)

P	Brière	NP1	Logistic	Logan	NP2
1	$T_m = 27.2$	$T_m = 31.0$	$T_m = 27.1$	$T_m = 29.3$	$T_m = 30.0$
2	$T_b = 11.4$	$T_b = 10.0$	$T_b = 15.0$	$T_b = 4.70$	$T_b = 6.13$
3	$r_{max} = 0.0197$	$T_1 = 24.0$	$\Delta_m = 1.05$	$\Delta_m = 5.50$	$T_1 = 14.5$
4		$r_{max} = 0.0205$	$\Delta_b = 0.934$	$\omega = 0.104$	$T_2 = 23.3$
5			$r_{max} = 0.0161$	$\Psi = 0.0076$	$r_1 = 0.0058$
6					$r_{max} = 0.0191$
σ	0.0009	0.0020	0.009	0.0009	0.0010
AIC	179.7	191.4	183.0	198.4	196.3
P	4	5	6	6	7

Table 3. Parameters for Tree 1 adult development rate curves. The estimated variance of development rates is given by σ. We calculate *r*max = 0.0173 for the Logan curve (not an estimated parameter for this curve).

P	Brière	NP1	Logistic	Logan	NP2
1	$T_m = 26.1$	$T_m = 27.9$	$T_m = 24.7$	$T_m = 25.9$	$T_m = 28.6$
2	$T_b = 12.7$	$T_b = 13.0$	$T_b = 16.1$	$T_b = 6.55$	$T_b = 9.38$
3	$r_{max} = 0.0216$	$T_1 = 21.1$	$\Delta_m = 0.9000$	$\Delta_m = 5.01$	$T_1 = 13.8$
4		$r_{max} = 0.0240$	$\Delta_b = 0.9000$	$\omega = 0.141$	$T_2 = 21.1$
5			$r_{max} = 0.0200$	$\Psi = 0.0135$	$r_1 = 0.0060$
6					$r_{max} = 0.0192$
σ	0.0013	0.0012	0.013	0.0025	0.0025
AIC	146.4	146.45	146.9	161.6	161.0
P	4	5	6	6	7

Table 4. The percentage of pairwise bootstraps (of 1,500) for which the AIC value was greater as well as significantly greater (ΔAIC > 5) than the corresponding Brière bootstrap for each adult development rate curve, for both trees

	Pairwise %		% Significant	
Model	Tree 2	Tree 1	Tree 2	Tree 1
Logistic	98.27	78.40	6.47	27.47
NP1	96.27	78.60	14.00	32.93

Table 5. NLL values for each tree using the fitted parameters for the Brière adult development rate curve, as well as those calculated via cross-validation. For example, the NLL in the lower left corner reflects predictions using Tree 2 parameters compared with emergence data from Tree 1

	Predicting Emergence From	
Parameterized Using	Tree 1	Tree 2
Tree 1	136.5	296.0
Tree 2	161.2	169.7

a standard deviation of 1.65 °C). The difference varies seasonally but is largest in the summer, when adult MPB are typically developing.

Deviances Have Laplace Distribution

The nominal AIC values (values for unbootstrapped data and the Briere rate curve) are $AIC_{Laplace} = 179.71$, $AIC_{Normal} = 193.61$, and $AIC_{Poisson} = 231.24$. Calculating the ΔAIC between the distributions (with ΔAIC > 5, corresponding to an odds ratio >10, as the difference we consider to be significant improvement, as in Burnham 2002), the Laplace distribution ΔAIC values are 13.89 for the Normal distribution and 51.53 for Poisson distribution, indicating that the Laplace distribution better describes the deviances in the context of the data, which is confirmed by the bootstrapped data. All of the bootstrapped Laplace AIC values were less than the nominal Poisson AIC, and 99.4% of the normal AIC values are smaller, meaning that in almost all bootstrapped samples the Laplace and normal deviance models outperformed Poisson (Supplementary Fig. S3A).

The Laplace and Normal bootstrapped AIC values are much more competitive. Considering bootstrapped resampling of the data, only 41.1% of the bootstrapped Normal AIC values are smaller than the nominal Laplace AIC, as opposed to 91.3% of the bootstrapped Laplace AIC values being smaller than the nominal Normal AIC (Supplementary Fig. S3B). Comparing individual bootstraps pairwise, 99.6% of Laplace AIC values are smaller than the m corresponding Normal AIC value. Therefore, we use a Laplace distribution for adult developmental rate curve selection.

Development Rate Curve Selection for Adults

Adult rate curve parameters are fit by minimizing Laplace NLL (equation 16) for all 5 candidate rate models using data from Tree 1 and Tree 2. We attempted to fit rate curves simultaneously to both trees, but common curves could not be fit across both trees reliably. We, therefore, use bootstrapped distributions and cross-validation to assess the suitability of parameters, considering each tree separately. Temperature thresholds and maximum rates vary among the rate curves, but the curves agree generally on beetle thermal response, particularly at inflection points (Fig. 2). Nominal parameters for the various rate curves appear in Table 2 (Tree 2) and Table 3 (Tree 1). For both trees, the Brière rate curve had the smallest nominal AIC value (Supplementary Fig. S4), though not always significantly so (i.e., ΔAIC > 5).

For Tree 2, we find a nonsignificant ΔAIC = 3.38 between the Brière curve and the Logistic curve, which has the next lowest nominal

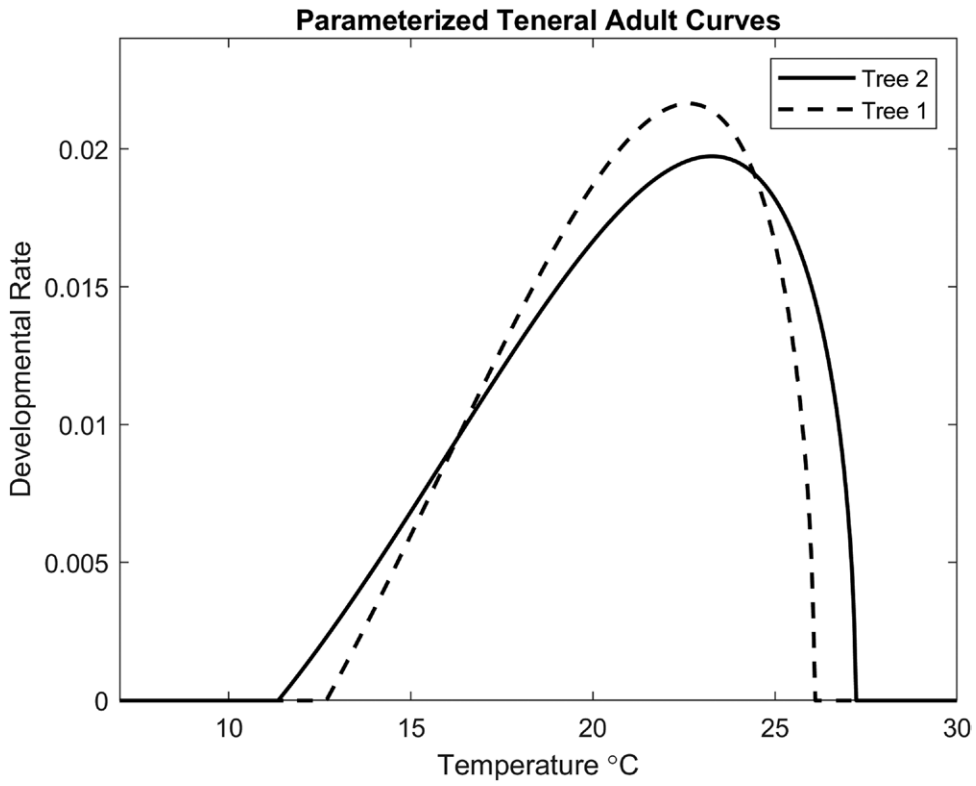

Fig. 3. Adult development rate fit to Brière curves using adult emergence data for Tree 1 (dashed) and Tree 2 (solid).

AIC value. The Brière curve was significantly better than all other curves tested for Tree 2 (Supplementary Fig. S4A). The ΔAIC for the Tree 1 Brière curve is not significantly better than either the NP1 and Logistic curves, which all have AIC slightly above 146 (Table 3). The Tree 1 Brière, NP1, and Logistic curves all have ΔAIC > 5 in comparison to the Logan and NP2 curves (Supplementary Fig. S4B), and we therefore remove the NP2 and Logan curves from consideration.

A simple pairwise comparison of Brière AIC values to NP1 and Logistic AIC values for the same bootstrap sample is overwhelmingly in favor of the Brière curve (Table 4); the Brière curve had lower AIC over 96% of the time for Tree 2 and over 78% of the time for Tree 1. However, only a fraction of these were significant improvements (that is, ΔAIC > 5). For Tree 2, the ΔAIC was at least 5 for 14.00% of the NPl bootstrap AIC values and 6.47% of the Logistic AIC values. For Tree 1, the ΔAIC was at least 5 for 32.93% of the NP1 bootstrap AIC values and 27.47% of the Logistic AIC values. This supports the picture presented by comparison of nominal AIC values (Tables 2 and 3) that the Brière curve is the best rate curve to describe adult development.

Parameter Value Selection for Brière Development Rate Curve

Attempts to fit emergence data for both trees simultaneously to the Brière rate curve with a common set of parameters were not convergent. Instead, we fit each tree separately and then cross-validated by calculating the NLL for each tree using the parameters fit to the emergence data of the other tree (Table 5). Tree 2 parameters have larger NLL than the Tree 1 parameters using the Tree 1 field data as input, but Tree 1 parameters perform poorly with Tree 2 observations. Although the parameterized rate curves for the 2 trees are similar (Fig. 3), the differences in parameters result in a notable change in cumulative emergence distributions, particularly in the south aspect (Fig. 4A). MPB peak emergence on the south aspect of Tree 2 was more accurately predicted with Tree 2 parameters than Tree 1 parameters (Fig. 4B). Considering confidence in parameters, the 90% confidence intervals are much broader for Tree 1 parameters in all cases, indicating that the fits are less reliable (Fig. 5). Due to the more successful cross-validation and tighter confidence intervals, we choose the parameters based on Tree 2 emergence data (Table 2, first column) for predicting MPB adult development in the AZ population.

Model Evaluation

Predictions using the Brière curve, parameterized with Tree 2 data (Table 2, first column), are compared with observations of adult emergence from Tree 3. The Brière rate curve with Tree 2 parameters predicts median and peak MPB adult emergence on the Tree 3 north bole aspect within a few days of observed median and peak emergence (Fig. 6A). The predicted emergence timing is similarly close to 10%–90% of total emergence completed. Although nearly all emergence from the south bole aspect of Tree 3 occurred over 2 observations, predicted and observed median emergence dates are only 1 wk apart (Fig. 6B).

We are also interested in comparing the AZ MPB adult development rate estimated herein with the adult rate estimated previously for the more northern UT MPB (Régnière et al. 2012). Laboratory data for this population was fit using equation (1) under the assumption of log-normal variance. We compare maximum development rate and range of development temperatures for the curve calibrated for the UT MPB population and the Brière developmental rate curve chosen above for the AZ population. Max development rate, r_{max}, is not an explicit parameter in (1), so we calculate it numerically using parameters from Regniere et al. (2012), yielding $r_{max} = 0.0752$ for the UT population. Taking into account the multiplicative log-normal variance to estimate the lowest reasonable limit for max development

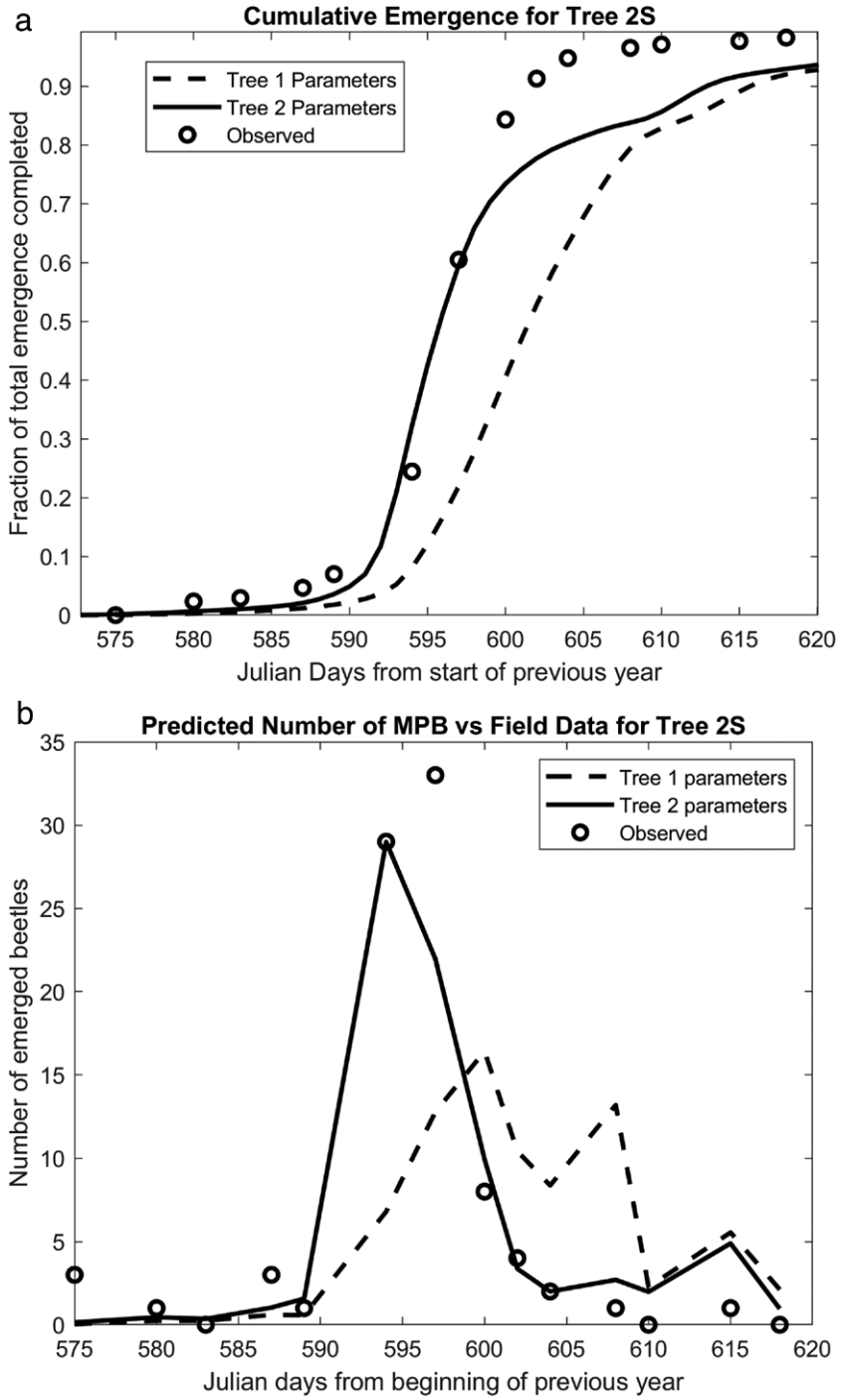

Fig. 4. Cross-validation results comparing A) observed cumulative adult emergence for Tree 2 south aspect and predictions using Tree 1 (dashed) and Tree 2 (solid) Brière parameters, and B) timing of observed emergence from Tree 2 south aspect and predictions using Tree 1 (dashed) and Tree 2 (solid) Brière parameters.

rate of the UT population, we multiply r_{max} by $\exp(-\sigma_{\text{North}})$, where $\sigma_{\text{North}} = 0.190$, giving a minimum reasonable estimate of $r_{max} = 0.0621$ for the UT population. This is much higher than maximum developmental rate for the AZ population, which never exceeds 0.025 in any bootstrapped sample. Adult AZ MPB development also occurs within a narrower band of temperatures relative to that estimated for the UT population. The developmental range of the AZ population is bounded between 9.5 °C and 27.5 °C (taking the upper and lower ends of the 90% CI, see Fig. 5), whereas the upper and lower thresholds for development in the northern population were estimated at 35 °C and 4.24 °C (Régnière et al. 2012) (note that multiplicative log-normal variance does not adjust estimated temperature thresholds).

Potential for Bivoltinism

Bivoltinism (2 generations in year) in AZ MPB has not been observed in the field, even when the population was relocated to a lower elevation and warmer habitat than its source location in Lockett Meadow (Soderberg et al. 2021). There are at least 2 constraints to bivoltinism in MPB, even in a warming climate (Bentz and Powell 2014). One, the facultative prepual diapause restricts development

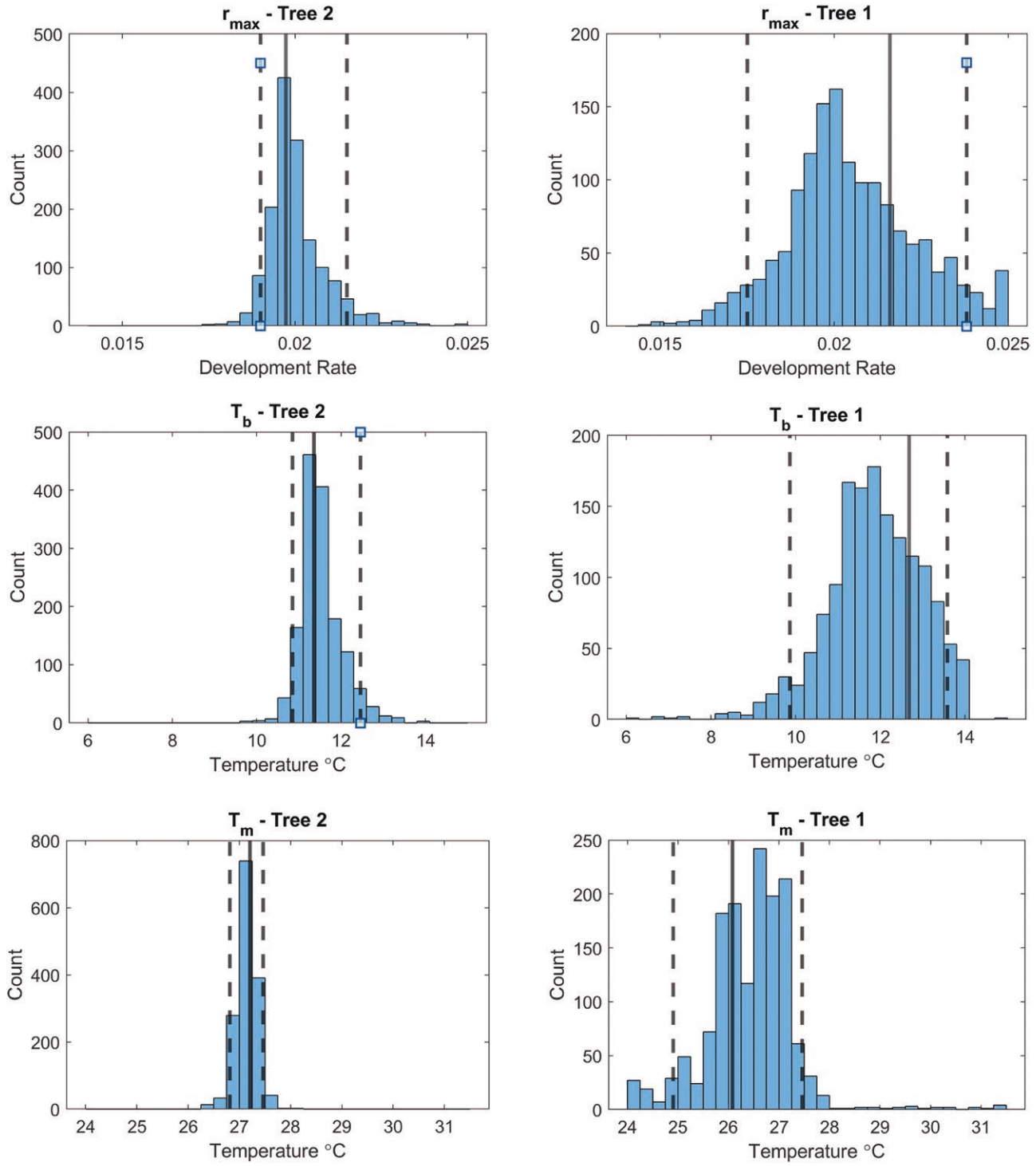

Fig. 5. Distributions of T_m, T_b, and r_{max} obtained from fitting parameters to 1,500 bootstraps of field emergence data for each tree, with nominal parameter lines in solid and 90% confidence interval bounds in dashed.

progression to the pupal stage and ultimately teneral adult when temperatures are below 15 °C (Bentz and Hansen 2018). Two, MPB eggs and pupae have evolved to be the least tolerant of cold temperatures (Bleiker et al. 2017, Bleiker and Smith 2019), and mortality would incur if generation timing was such that these lifestages were present during winter. To test for bivoltinism in a warming climate, we used the observed mean of north and south bole aspect phloem temperatures in Tree 2 for the 2015–2016 MPB generation as a base and incrementally increased mean temperature. Using observed attack timing for the 2015–2016 generation as the initial condition, the median date of emergence for a potential second generation is calculated using the output of the first generation as input for the second.

Median adult emergence with no mean temperature added reflects the emergence of the univoltine generation in August of the following year. As the mean temperature increased, the median

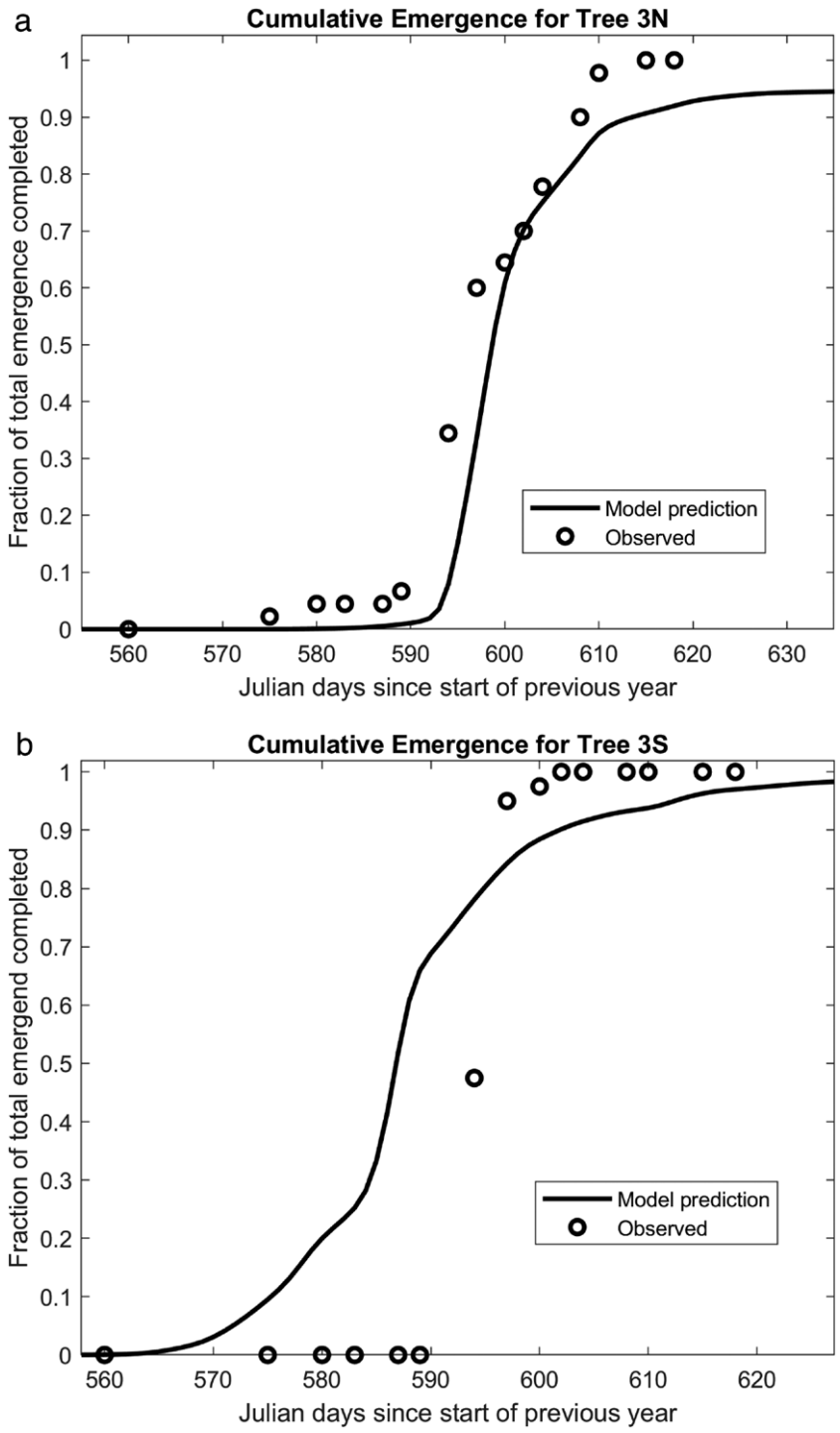

Fig. 6. The cumulative fraction of total adult emergence observed in the field (circles) and predicted by the model (solid) for Tree 3 north bole aspect A) and south bole aspect B).

day for the emergence of second-generation brood adults initially occurred increasingly earlier and eventually in the same year as first-generation adult emergence (see Fig. 7). The earliest date of median, second-generation adult emergence is 30 October when 5.0–5.5 °C is added; for higher mean temperatures, the median date of second-generation adult emergence shifts later. However, emergence in late October is unlikely to be seasonally appropriate. Even with 5.5 °C warming of hourly winter temperatures measured during our study period, eggs would encounter temperatures that could cause significant mortality (Bleiker et al. 2017). Additionally, as mean temperature increases beyond 5 °C, the emergence timing of brood adults is projected to occur later in the year as temperatures exceed optimal development rates of preadult (McManis et al. 2018) and adult lifestages, resulting in a delay rather than speeding up of overall development. We acknowledge that temperatures associated with climate change are variable at multiple temporal scales and not directly comparable to simple increases in the mean we used for this scenario.

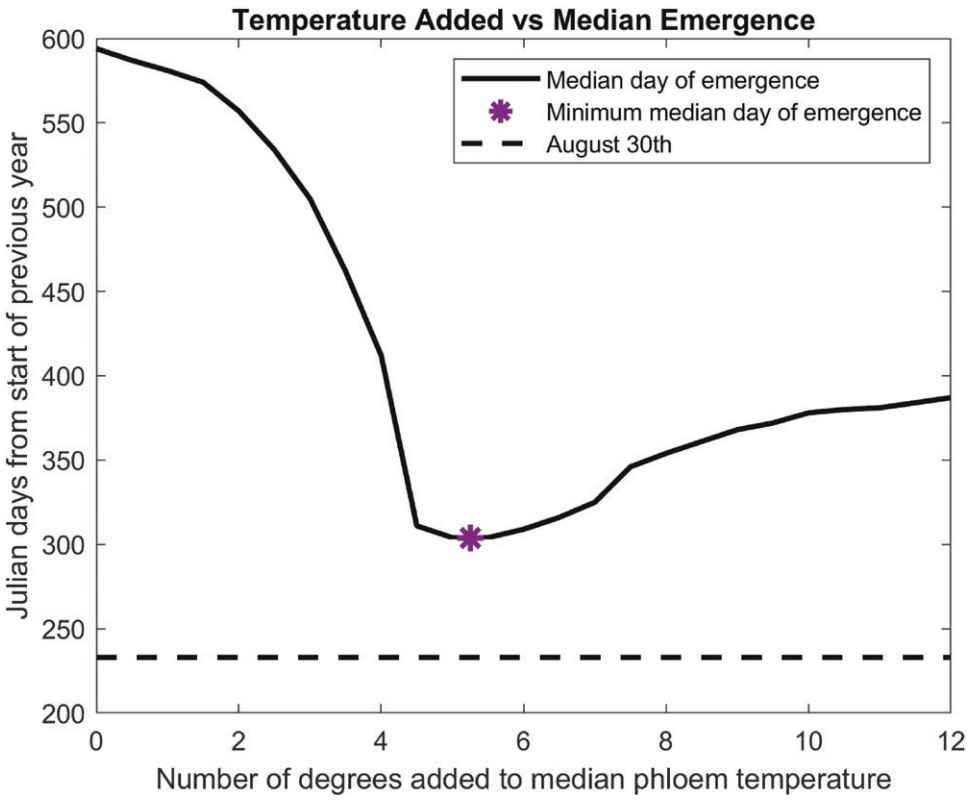

Fig. 7. Median date of a second period of adult emergence in a single year (bivoltine) using the parameterized adult development rate curve for Arizona MPB. Phloem temperatures were measured in the field and sequentially increased to drive the model, using the output of 1 generation as input for the second generation. The Julian day for August 30 is indicated by the dashed line.

Discussion and Conclusion

Clinal genetic and plastic variation in developmental parameters reflects adaptation to local climates and is common in insect species with broad geographic ranges (Roff 1990). The adult development rate curve we estimate for the AZ population differs significantly from that estimated previously for the more northern UT population (Régnière et al. 2012). The lowest value of maximum development, r_{max}, estimated for the northern UT population was 0.0622, which is much higher than the rate we estimated for the AZ population, which did not exceed 0.025 in any bootstrapped sample. Our results corroborate previous research (McManis et al. 2018, Soderberg et al. 2021), highlighting that the difference in generation time between the two geographically separated populations is due to evolved and slower adult development in the warmer habitat of the AZ MPB population. The longer generation time of the AZ population, relative to the more northern UT, likely results from selection pressure to maintain univoltinism in a warmer climate (Bracewell et al. 2013, Soderberg et al. 2021, Bentz et al. 2022). Conserved univoltine responses within a species across latitudes have been observed in other insect species (Śniegula et al. 2016, Kong et al. 2019).

Although a reduction in generation time with warming is often expected, plastic physiological responses, including dormancy strategies such as diapause and quiescence, can either maintain or increase generation time with warming (Forrest 2016). Indeed, an adult dormancy was recently identified in MPB (Hansen et al., submitted), and manifestation was found to differ among populations within haplogroups that formed following Pleistocene glaciation (Dowle et al. 2017). The AZ population analyzed herein is in the haplogroup shown to have an adult dormancy that is induced by relatively high temperatures and averted by cool temperatures (Hansen et al., submitted). In contrast, adult dormancy was low or absent in a population from southern Idaho that resides in a separate haplogroup that also includes northern UT. Our result of slow development time (i.e., reduced rate) in AZ adults, relative to northern UT, provides additional corroboration for an adult dormancy in MPB that varies geographically.

At the southern limit of its distribution in AZ MPB outbreaks are rare. MPB can be found at relatively high elevations, including our study site, but is limited or absent in lower elevation AZ Pinus forests (McHugh et al. 2003, Gaylord et al. 2006, Williams et al. 2008). The number and pattern of MPB attacking baited trees in our study were at the low end of the range of attacks observed in a previous field study but with similar timing and pattern of attacks and emergence (Bentz et al. 2014). The number of brood adults emerging, however, was less than previously observed (Bentz et al. 2014). It is unclear what factors influenced beetle mortality, limiting total emergence and forcing emergence variability among our study trees. Potential contributing factors include lethal winter temperatures (Supplementary Fig. S2) and direct and indirect effects of locally adapted and varying ectosymbionts, including phoretic mites and fungi (Vissa et al. 2020, Hofstetter et al. 2022). We acknowledge the low sample size used to parameterize models and encourage the collection of additional field data to be used in conjunction with our novel modeling strategy to evaluate potential variability in population-level estimates.

Although a summer MPB generation can occur (Reid 1962, Mitton and Ferrenberg 2012, Bentz et al. 2014), bivoltinism has not been observed in MPB (Bentz and Powell, 2014, Soderberg et al.

2021). Due to the ecological and economic effects of *Pinus* mortality, however, 2 generations of MPB would be a harbinger of a catastrophic regime change for MPB (Bentz and Powell 2014). Shorter generation time could lead to increased population growth and subsequently, increased tree mortality. Although bivoltinism was previously hypothesized to manifest in a warming climate (Bentz et al., 2016), our results using the estimated adult rate curve for AZ MPB, with previously described preadult lifestage development rates, suggest that attempts for a second generation in a single-year would be unsuccessful due to developmental traps, even with the warming of mean phloem temperatures up to 5.5 °C. Climate change will undoubtedly affect MPB seasonality, and it is clear that responses will be complex and differ across its range. Our results highlight that recognizing and describing evolved life history responses will be required to adequately predict population success and range expansion in a changing climate.

Acknowledgments

We thank John Anhold, Danny DePinte, Monica Gaylord, Amanda Grady, Matt Hansen, Rich Hofstetter, Anne McManis and Jim Vandygriff for data collection. The use of trade or firm names in this paper is for reader information only and does not imply endorsement by the U.S. Department of Agriculture of any product or service. The findings and conclusions in this publication are those of the authors and should not be construed to represent any official USDA or U.S. Government determination or policy.

Author contributions

Catherine Wangen (Formal analysis [lead], Methodology [lead], Software [lead], Visualization [lead], Writing—original draft [lead], Writing—review & editing [supporting]), Jim Powell (Conceptualization [equal], Project administration [lead], Supervision [lead], Writing—review & editing [lead]), and Barbara Bentz (Conceptualization [equal], Data curation [lead], Funding acquisition [lead], Resources [lead], Writing—review & editing [supporting])

Supplementary data

Supplementary data are available at *Journal of Insect Science* online.

Funding

This research was supported by funding from the USDA Forest Service, Forest Health Protection Special Technology Development Program R3-2015-04.

References

Addison A, Powell JA, Bentz BJ, et al. 2015. Integrating models to investigate critical phenological overlaps in complex ecological interactions: the mountain pine beetle-fungus symbiosis. J. Theor. Biol. 368:55–66. https://doi.org/10.1016/j.jtbi.2014.12.011

Bentz BJ, Hansen EM. 2018. Evidence for a prepupal diapause in the mountain pine beetle (*Dendroctonus ponderosae*). Environ. Entomol. 47(1):175–183. https://doi.org/10.1093/ee/nvx192

Bentz B, Mullins D. 1999. Ecology of mountain pine beetle (Coleoptera: Scolytidae) cold hardening in the intermountain west. Environ. Entomol. 28(4):577–587.

Bentz BJ, Powell JA. 2014. Mountain pine beetle seasonal timing and constraints to bivoltinism: a comment on Mitton and Ferrenberg, 'Mountain pine beetle develops an unprecedented summer generation in response to climate warming'. Am. Nat. 184(6):787–796. https://doi.org/10.1086/678405

Bentz BJ, Logan JA, Amman GD. 1991. Temperature-dependent development of the mountain pine beetle (Coleoptera: Scolytidae) and simulation of its phenology. Can. Entomol. 123(5):1083–1094. https://doi.org/10.4039/ent1231083-5

Bentz BJ, Logan JA, Vandygriff JC. 2001. Latitudinal variation in *Dendrocto ponderosae* (Coleoptera: Scolytidae) development time and adult size. Can. Entomol. 133(3):375–387. https://doi.org/10.4039/ent133375-3

Bentz B, Vandygriff J, Jensen C, et al. 2014. Mountain pine beetle voltinism and life history characteristics across latitudinal and elevational gradients in the western united states. Forest Sci. 60(3):434–449. https://doi.org/10.5849/forsci.13-056

Bentz BJ, Jonsson AM, Schroeder M, et al. 2019. *Ips typographus* and *Dendroctonus ponderosae* models project thermal suitability for intra- and inter-continental establishment in a changing climate. Front. For. Glob. Change 2(1):1–17. https://doi.org/10.3389/ffgc.2019.00001

Bentz BJ, Duncan JP, Powell JA. 2016. Elevational shifts in thermal suitability for mountain pine beetle population growth in a changing climate. Forestry 89(3):271–283. https://doi.org/10.1093/forestry/cpv054

Bentz BJ, Hansen EM, Davenport M, et al. 2022. Complexities in predicting mountain pine beetle and spruce beetle response to climate change. In: Bark beetle management, ecology, and climate change. Academic Press: Elsevier; p. 31–54.

Bleiker K, Smith G. 2019. Cold tolerance of mountain pine beetle (Coleoptera: Curculionidae) pupae. Environ. Entomol. 48(6):1412–1417.

Bleiker KP, Smith GD, Humble LM. 2017. Cold tolerance of mountain pine beetle (Coleoptera: Curculionidae) eggs from the historic and expanded ranges. Environ. Entomol. 46(5):1165–1170. https://doi.org/10.1093/ee/nvx127

Bonhomme R. 2000. Bases and limits to using 'degree-day' units. Eur. J. Agron. 13(1):1–10. https://doi.org/10.1016/s1161-0301(00)00058-7

Bracewell RR, Pfrender ME, Mock KE, et al. 2013. Contrasting geographic patterns of genetic differentiation in body size and development time with reproductive isolation in *Dendroctonus ponderosae* (Coleoptera: Curculionidae, Scolytinae). Ann. Entomol. Soc. Am. 106(3):385–391. https://doi.org/10.1603/an12133

Brière J-F, Pracros P, Le Roux A-Y, et al. 1999. A novel rate model of temperature-dependent development for arthropods. Environ. Entomol. 28(1):22–29.

Burnham K. Model selection and multimodel inference: a practical information-theoretic approach. New York: Springer; 2002.

Danilevskii AS. Photoperiodism and seasonal development of insects. Edinburgh, UK: Oliver & Boyd Ltd; 1965.

Davídková M, Doležal P. 2019. Temperature-dependent development of the double-spined spruce bark beetle *Ips duplicatus* (Sahlberg, 1836) (Coleoptera: Curculionidae). Agric. For. Entomol. 21(4):388–395. https://doi.org/10.1111/afe.12345

Davidson J. 1944. On the relationship between temperature and rate of development of insects at constant temperatures. J. Anim. Ecol. 13(1):26–38. https://doi.org/10.2307/1326

Denlinger D. 2002. Regulation of diapause. Annu. Rev. Entomol. 47(1):93–122.

Dowle EJ, Bracewell RR, Pfrender ME, et al. 2017. Reproductive isolation and environmental adaptation shape the phylogeography of mountain pine beetle *Dendroctonus ponderosae*. Mol. Ecol. 26(21):6071–6084. https://doi.org/10.1111/mec.14342

Forrest JR. 2016. Complex responses of insect phenology to climate change. Curr. Opin. Insect Sci. 17:49–54. https://doi.org/10.1016/j.cois.2016.07.002

Gaylord M, Kolb T, Wallin K, et al. 2006. Seasonality and lure preference of bark beetles (Curculionidae: Scolytinae) and associates in a northern Arizona ponderosa pine forest. Environ. Entomol. 35(1):37–47.

Gilbert E, Powell J, Logan J, et al. 2004. Comparison of three models predicting developmental milestones given environmental and individual variation. Bull. Math. Biol. 66(6):1821–1850. https://doi.org/10.1016/j.bulm.2004.04.003

Grist EP, Gurney WS. 1995. Stage-specificity and the synchronisation of life-cycles to periodic environmental variations. J. Math. Biol. 34:123–147.

Gurney WSC, Crowley PH, Nisbet RM. 1994. Stage-specificity and the synchronisation of life-cycles to periodic environmental variations. Theor. Popul. Biol. 46(3):319–343.

Hansen EM, Bentz BJ, Powell JA, et al. 2011. Prepupal diapause and instar IV developmental rates of the spruce beetle, *Dendroctonus rufipennis* (Coleoptera: Curculionidae, Scolytinae). J. Insect Physiol. 57(10):1347–1357. https://doi.org/10.1016/j.jinsphys.2011.06.011

Hofstetter RW, Klepzig KD, Villari C. 2022. Effects of rising temperatures on ectosymbiotic communities associated with bark and ambrosia beetles. In: Bark beetle management, ecology, and climate change. Academic Press; p. 303–341.

Honek A. 1996. The relationship between thermal constants for insect development: verification. Acta Soc. Zool. Bohem. 60:115–152.

Kong JD, Hoffmann AA, Kearney MR. 2019. Linking thermal adaptation and life-history theory explains latitudinal patterns of voltinism. Philos. Trans. R. Soc. London, Ser. B 374(1778):20180547. https://doi.org/10.1098/rstb.2018.0547

Logan JA, Bentz BJ. 1999. Model analysis of mountain pine beetle (Coleoptera: Scolytidae) seasonality. Environ. Entomol. 28(6):924–934. https://doi.org/10.1093/ee/28.6.924

Logan JA, Powell JA. 2001. Ghost forests, global warming, and the mountain pine beetle (Coleoptera: Scolytidae). Am. Entomol. 47(3):160–173. https://doi.org/10.1093/ae/47.3.160

Logan JA, Wollkind DJ, Hoyt SC, et al. 1976. An analytic model for description of temperature dependent rate phenomena in arthropods. Environ. Entomol. 5(6):1133–1140. https://doi.org/10.1093/ee/5.6.1133

Masaki S. 1980. Summer diapause. Annu. Rev. Entomol. 25(1):1–25. https://doi.org/10.1146/annurev.en.25.010180.000245

McHugh CW, Kolb TE, Wilson JL. 2003. Bark beetle attacks on ponderosa pine following fire in northern Arizona. Environ. Entomol. 32(3):510–522. https://doi.org/10.1603/0046-225x-32.3.510

McManis AE, Powell JA, Bentz BJ. 2018. Developmental parameters of a southern mountain pine beetle (Coleoptera: Curculionidae) population reveal potential source of latitudinal differences in generation time. Can. Entomol. 151(1):1–15. https://doi.org/10.4039/tce.2018.51

McManis AE, Powell JA, Bentz BJ. 2019. Modeling mountain pine beetle (*Dendroctonus ponderosae*) oviposition. Entomol. Exp. Appl. 167(5):457–466. https://doi.org/10.1111/eea.12783

Mitton J, Ferrenberg S. 2012. Mountain pine beetle develops an unprecedented summer generation in response to climate warming. Am. Naturalist 179(5):E163–E171.

Powell J, Bentz B. 2009. Connecting phenological predictions with population growth rates for mountain pine beetle, an outbreak insect. Landsc. Ecol. 24(5):657–672.

Powell J, Logan J. 2005. Insect seasonality: circle map analysis of temperature-driven life cycles. Theor. Popul. Biol. 67(3):161–179.

Rebaudo F, Rabhi V-B. 2018. Modeling temperature-dependent development rate and phenology in insects: review of major developments, challenges, and future directions. Entomol. Exp. Appl. 166(8):607–617. https://doi.org/10.1111/eea.12693

Régnière J, Powell J. 2013. Animal life cycle models (poikilotherms). In: Phenology: an integrative environmental science. Dordrecht, Netherlands: Springer; p. 295–316.

Régnière J, Powell J, Bentz B, et al. 2012. Effects of temperature on development, survival and reproduction of insects: experimental design, data analysis and modeling. J. Insect Physiol. 58(5):634–647. https://doi.org/10.1016/j.jinsphys.2012.01.010

Reid RW. 1962. Biology of the mountain pine beetle, *dendroctonus monticolae* Hopkins, in the east Kootenay region of British Columbia I. life cycle, brood development, and flight periods. Can. Entomol. 94(5):531–538. https://doi.org/10.4039/ent94531-5

Roff D. 1990. Understanding the evolution of insect life-cycles: the role of genetic analysis. In: Insect life cycles: genetics, evolution and co-ordination. London: Springer; p. 5–27.

Safranyik L, Linton D. 1991. Unseasonably low fall and winter temperatures affecting mountain pine beetle and pine engraver beetle populations and damage in the British Columbia Chilcotin region. J. Entomol. Soc. B.C. 88:17–21.

Śniegula S, Golab M, Johansson F. 2016. Time constraint effects on phenology and life history synchrony in a damselfly along a latitudinal gradient. Oikos 125(3):414–423.

Soderberg D, Mock K, Hofstetter R, et al. 2021. Translocation experiment reveals capacity for mountain pine beetle persistence under climate warming. Ecol. Monogr. 91(1):1-19.

Tauber C, Tauber M. 1986. Ecophysiological responses in life-history evolution: Evidence for their importance in a geographically widespread insect species complex. Can. J. Zool. 64(4):875–884.

Vissa S, Mercado J, Malesky D, et al. 2020. Patterns of diversity in the symbiotic mite assemblage of the mountain pine beetle, *Dendroctonus ponderosae* Hopkins. Forests 11(10):1102.

Wangen C. 2021. A phenological model for a southern population of mountain pine beetle [Master's thesis]. Utah State University.

Wangen C, Powell J, Bentz B. 2022. Oviposition model for a southern population of mountain pine beetle. Bull. Math. Biol. 84(133):133.

Williams K, McMillin J, DeGomez T, et al. 2008. Influence of elevation on bark beetle community structure in ponderosa pine stands of north-central Arizona. Environ. Entomol. 37:94–109.